

# Measurement of activation cross sections of alpha particle induced reactions on iridium up to an energy of 50 MeV

S. Takács<sup>a,\*</sup>, F. Ditrói<sup>a</sup>, Z. Szűcs<sup>a</sup>, M. Aikawa<sup>b</sup>, H. Haba<sup>c</sup>, Y. Komori<sup>c</sup>, M. Saito<sup>d</sup>

<sup>a</sup> Institute for Nuclear Research, Hungarian Academy of Sciences, 4026 Debrecen, Hungary

<sup>b</sup> Faculty of Science, Hokkaido University, Sapporo 060-0810, Japan

<sup>c</sup> Nishina Center for Accelerator-Based Science, RIKEN, Wako 351-0198, Japan

<sup>d</sup> Graduate School of Biomedical Science and Engineering, Hokkaido University, Sapporo 060-8638, Japan

## HIGHLIGHTS

- Activation cross sections of alpha particle induced reactions were measured on natural iridium target.
- Stacked target technique and activation method was used.
- High resolution gamma spectrometry without chemical separation was used to activity determination.
- Activation cross sections for gold, platinum and iridium isotopes ( $^{196\text{m}2}\text{Au}$ ,  $^{196\text{m}}\text{Au}$ ,  $^{195\text{m}}\text{Au}$ ,  $^{194}\text{Au}$ ,  $^{193\text{m}}\text{Au}$ ,  $^{192}\text{Au}$ ,  $^{191\text{m}}\text{Au}$ ,  $^{191}\text{Pt}$ ,  $^{195\text{m}}\text{Pt}$ ,  $^{194\text{g}}\text{Ir}$ ,  $^{194\text{m}}\text{Ir}$ ,  $^{192\text{g}}\text{Ir}$ ,  $^{190\text{g}}\text{Ir}$  and  $^{189}\text{Ir}$ ) were determined.
- Production possibility of  $^{195\text{m}}\text{Pt}$  with high specific activity is discussed.

## ARTICLE INFO

### Keywords:

Platinum- $^{195\text{m}}\text{Pt}$   
 $\alpha$ -particle irradiation  
 Iridium target  
 Cross section  
 Excitation function

## ABSTRACT

Cross sections of alpha particle induced nuclear reactions on iridium were investigated using a 51.2-MeV alpha particle beam. The standard stacked-foil target technique and the activation method were applied. The activity of the reaction products was assessed without chemical separation using high resolution gamma-ray spectrometry. Excitation functions for production of gold, platinum and iridium isotopes ( $^{196\text{m}2}\text{Au}$ ,  $^{196\text{m}}\text{Au}$ ,  $^{195\text{m}}\text{Au}$ ,  $^{194}\text{Au}$ ,  $^{193\text{m}}\text{Au}$ ,  $^{192}\text{Au}$ ,  $^{191\text{m}}\text{Au}$ ,  $^{191}\text{Pt}$ ,  $^{195\text{m}}\text{Pt}$ ,  $^{194\text{g}}\text{Ir}$ ,  $^{194\text{m}}\text{Ir}$ ,  $^{192\text{g}}\text{Ir}$ ,  $^{190\text{g}}\text{Ir}$  and  $^{189}\text{Ir}$ ) were determined and compared with available earlier measured experimental data and results of theoretical calculations using TALYS code system. Cross section data were reported for the first time for the  $^{\text{nat}}\text{Ir}(\alpha, x)^{196\text{m}2}\text{Au}$ ,  $^{\text{nat}}\text{Ir}(\alpha, x)^{196\text{m}}\text{Au}$ ,  $^{\text{nat}}\text{Ir}(\alpha, x)^{191}\text{Pt}$ ,  $^{\text{nat}}\text{Ir}(\alpha, x)^{195\text{m}}\text{Pt}$ ,  $^{\text{nat}}\text{Ir}(\alpha, x)^{194\text{g}}\text{Ir}$ ,  $^{\text{nat}}\text{Ir}(\alpha, x)^{194\text{m}}\text{Ir}$ ,  $^{\text{nat}}\text{Ir}(\alpha, x)^{190\text{g}}\text{Ir}$  and  $^{\text{nat}}\text{Ir}(\alpha, x)^{189}\text{Ir}$  processes. A possible production route for  $^{195\text{m}}\text{Pt}$ , the potentially important radionuclide in nuclear medicine, is discussed.

## 1. Introduction

The aim of this work was two folded, to investigate in general the excitation functions of alpha particle induced nuclear reactions on iridium target to get reliable experimental data for different applications using thin Ir target foils with natural isotopic composition and to investigate the  $^{\text{nat}}\text{Ir}(\alpha, x)^{195\text{m}}\text{Pt}$  production route to produce high specific activity  $^{195\text{m}}\text{Pt}$  for medical applications. In recent years, low-energy electron emitter radioisotopes gained considerable significance in use of different medical applications. The  $^{195\text{m}}\text{Pt}$  is one of those radionuclides having proper nuclear characteristics for internal therapy investigations ( $T_{1/2} = 4.03\text{d}$ ,  $IT = 100\%$ ,  $E_{\gamma} = 98.9\text{keV}$ ,  $I_{\gamma} = 11.4\%$ ). Due to the low energy of the emitted conversion and Auger electrons their energy is deposited in a very short range which concentrates large part of the

decay-energy in a small volume, preferably in a single targeted cell. The range of Auger and conversion electrons is so short that their cytotoxicity has some effect only if they are incorporated in the cell's DNA or in the immediate vicinity of the nucleus of a cell. Therefore, the use of  $^{195\text{m}}\text{Pt}$  has much more relevance in imaging the biodistribution of cisplatin and other cytotoxic platinum compounds than in the cancer treatment (Aalbersberg et al., 2017). Its low energy gamma photons ( $E_{\gamma} = 98.9\text{keV}$ ) can be used for medical imaging. Thus, attaching or including  $^{195\text{m}}\text{Pt}$  into a Pt-compound enables imaging of the biodistribution of the compound using SPECT or gamma cameras. Beside the  $^{\text{nat}}\text{Ir}(\alpha, x)^{195\text{m}}\text{Pt}$  reaction this work provides for the first time systematic cross section data measured for the  $^{\text{nat}}\text{Ir}(\alpha, x)^{196\text{m}2}\text{Au}$ ,  $^{\text{nat}}\text{Ir}(\alpha, x)^{196\text{m}}\text{Au}$ ,  $^{\text{nat}}\text{Ir}(\alpha, x)^{191}\text{Pt}$ ,  $^{\text{nat}}\text{Ir}(\alpha, x)^{194\text{g}}\text{Ir}$ ,  $^{\text{nat}}\text{Ir}(\alpha, x)^{194\text{m}}\text{Ir}$ ,  $^{\text{nat}}\text{Ir}(\alpha, x)^{190\text{g}}\text{Ir}$  and  $^{\text{nat}}\text{Ir}(\alpha, x)^{189}\text{Ir}$  reactions up to 50 MeV alpha particle

\* Corresponding author.

E-mail address: [stakacs@atomki.hu](mailto:stakacs@atomki.hu) (S. Takács).

energy. The measured cross section data may contribute to the improvement of theoretical model codes. In this work our experimental results are compared to the results of the TALYS calculation, taken from the TENDL-2015 data library, for each of the reactions.

## 2. Experimental

### 2.1. Targets and irradiation

The iridium target foils (purity 99.9%) were purchased from Goodfellow Company, with nominal thickness of 25  $\mu\text{m}$  and size of 25 mm by 25 mm. Two foils with actual areal density of 57.036  $\text{mg}/\text{cm}^2$  and 54.279  $\text{mg}/\text{cm}^2$  were used. The average thickness of each Ir foil was calculated by measuring the weight and the surface area of the foil. The foils were cut up 8  $\times$  8 mm pieces and two stacks were constructed including the iridium foils interleaved with some Ti foils (10.9  $\mu\text{m}$  thick, Goodfellow, 99.99%) for monitoring the beam intensity and to decrease the beam energy. The two stacks were irradiated in a Faraday-cup like vacuum chamber equipped with a long collimator, assuring a negligible small solid angle for the escaping secondary electrons. The irradiations were performed at  $E_\alpha = 51.27$  MeV and  $E_\alpha = 51.23$  MeV primary alpha particle beam energies using the azimuthally varying field (AVF) cyclotron of the RIKEN RI Beam Factory, Wako, Japan. The initial beam energy was confirmed by time of flight measurement before and after the irradiation (Watanabe et al., 2014). The beam current was kept stable and constant during the irradiation.

The two stacks were irradiated for duration of 2.0 h and 1.0 h at the average beam intensities of  $I_\alpha = 209$  nA and  $I_\alpha = 207$  nA, respectively. The collected charge was recorded every minute to check the beam stability. Each stack contained 8 iridium foils and some Ti monitor foils to check the beam parameters as well as to shift the effective bombarding energy for the iridium target foils. The energy loss of the alpha particles passing through the layers of the stacked target was calculated by using the semi-empirical formula proposed by Ziegler (1978). A comparison of the recommended cross sections of the  $^{nat}\text{Ti}(\alpha, x)^{51}\text{Cr}$  monitor reaction and the recoil corrected experimental values deduced in this study is shown in Fig. 1. Determining the energy loss in the low energy part of the stack is more critical; therefore we used monitor foils in that section of the stack. The experimental cross sections and the recommended data (IAEA-TECDOC, 2001) are in good agreement indicating that the deduced beam parameters, the energy loss calculation, and the data deduction method are correct.

### 2.2. Gamma spectrometry measurements and data analysis

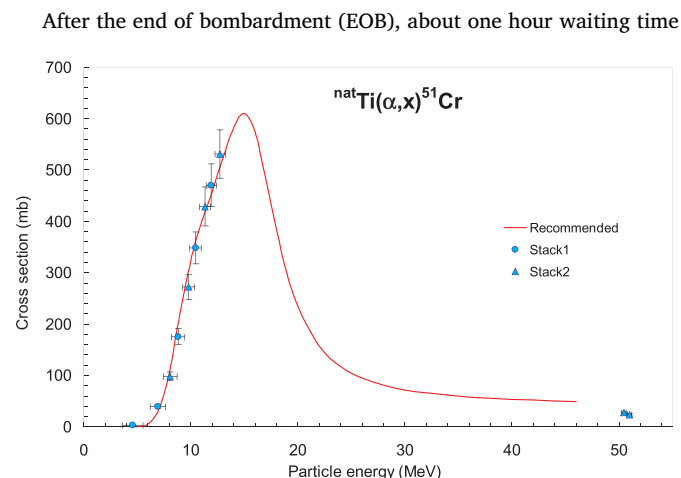


Fig. 1. Comparison of the recommended excitation function of the  $^{nat}\text{Ti}(\alpha, x)^{51}\text{Cr}$  monitor reaction and the experimental cross section data points deduced in this work for the two irradiated stacks.

was applied before separating the target foils from the stack. Each foil was enclosed in small, marked plastic bag for gamma-ray spectroscopic measurement. Using a high resolution HPGe gamma-ray spectrometer based on detector manufactured by Ortec Company (ORTEC GEM-25185-P and ORTEC GEM35P4-70) there was no need for chemical separation of the produced isotopes. Instead, several gamma-spectra were recorded for every irradiated foil with different waiting times. Four series of gamma measurements were performed for the iridium target foils to follow the decay of the produced radionuclides. It made possible to separate the contributions of different isotopes to a complex gamma peak. Since the 16 iridium foils were measured one by one each foil had different waiting time. In the first series of measurements the acquisition started about 1 h after EOB and the last foil in that series was measured after about 23 h waiting time. The second series of measurements was performed with waiting times between 24 h and 75 h after EOB and the applied measuring times were between 2 and 17 h. The third series were started after minimum 100 h of waiting time. The last series of measurements were performed after a two months of waiting time. The activity of the Ti monitor foils were assessed after a week of waiting time. The detector sample distance was set between 100 cm and 5 cm to keep the pileup effect and dead time of the electronics low, but each measurement in one series was done at the same detector-sample distance. The geometry dependent efficiency of the detector was determined for the used detector-sample distances by using calibrated mixed standard gamma-ray point source consisted of  $^{57,60}\text{Co}$ ,  $^{88}\text{Y}$ ,  $^{109}\text{Cd}$ ,  $^{113}\text{Sn}$ ,  $^{137}\text{Cs}$ ,  $^{139}\text{Ce}$  and  $^{241}\text{Am}$ . The net peak area of the photo-peaks in the spectra was calculated using the fitting algorithm included in the acquisition software packages. For separating complex peaks the FORGAMMA (Székely, 1985), an interactive peak analysis code, was used.

To estimate the total attenuation of a low energy gamma photons in the high density iridium target foil the well known attenuation equation and the attenuation coefficient taken from (Hubbell et al., 2004) was used. For the calculation, the foil was divided into 0.1  $\mu\text{m}$  layers and the attenuation of the gamma photons from a certain layer was calculated for every subsequent layers weighted by the activity distribution inside the foil. An average attenuation factor was calculated for every iridium target foil, which was then used to correct the derived cross section. The primary activity distribution inside the foil was estimated by using the non corrected excitation function, since only the relative amplitude of the cross sections is important to know.

For data evaluation the nuclear data (half-life, gamma-ray energy and intensity) were taken from NuDat2.7 (NuDat2.7) and are collected in Table 1, where only the gamma lines and their intensities used in the data analysis are tabulated. In the data analysis, to determine the activity of a certain produced isotope, not always the most intense gamma line was used by default, but an independent- and interference free gamma line was selected when it was possible. For each reaction the excitation function was estimated by using a cubic-spline algorithm over the deduced experimental data points.

### 2.3. Uncertainty of the experimental cross sections

The estimated total uncertainty of the deduced cross sections is from different sources of uncertainties. All partial uncertainties were rounded up by estimating their value on a conservative way. The following sources were considered:

The uncertainty of the average areal density and number of target nuclei/ $\text{cm}^2$  1%.

Uncertainty of the charge measurement of the bombarding particles 3%.

Uncertainty of the peak area determination 1–7%, for separation of complex peaks 15%.

Uncertainty of detector efficiency 3–6%.

Uncertainty of decay data (gamma intensity, half-life) 3%.

Download English Version:

<https://daneshyari.com/en/article/8208600>

Download Persian Version:

<https://daneshyari.com/article/8208600>

[Daneshyari.com](https://daneshyari.com)